ChemComm

Accepted Manuscript

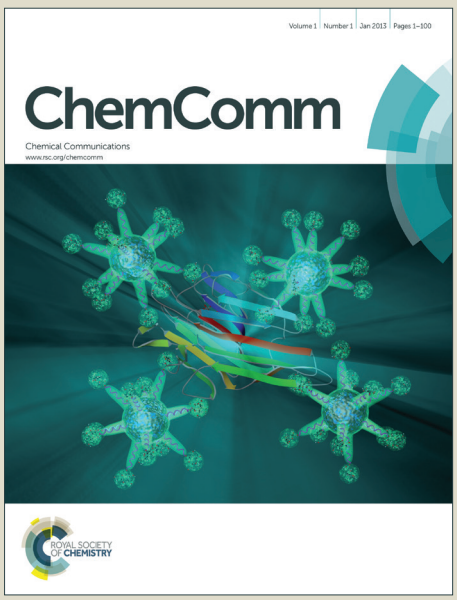

ROYAL SOCIETY OF CHEMISTRY

www.rsc.org/chemcomm

Journal Name

COMMUNICATION

Modulation of single-molecule magnet behaviour via photochemical [2+2] cycloaddition

Received 00th January 20xx,
Accepted 00th January 20xx

DOI: 10.1039/x0xx00000x

www.rsc.org/

Long-Fei Wang,[a] Jiang-Zhen Qiu,[a] Jun-Liang Liu,*[a] Yan-Cong Chen,[a] Jian-Hua Jia,*[a] Jesús Jover,[b] Eliseo Ruiz*[b] and Ming-Liang Tong*[a]

The first example of phototunable SMM has been reported. Upon UV irradiation, variations of coordination sphere around Dy(III) ions actually affect the magnetic behaviour of compound via [2+2] cycloaddition reaction, leading to a magnetic transformation from the SMM behaviour to a field-induced slow relaxation.

Single-molecule magnets (SMMs) have been becoming the focus of considerable research efforts due to their potential applications for high-density storage devices and quantum computations.[1] Heavy lanthanide ions, especially Dy(III) ion, have been commonly used for designing SMMs due to their inherent large magnetic anisotropy derived from large angular moments (*J*) as well as crystal-field effect.[2] Recently, Sessoli and co-workers studied the variation of coordination environment around Dy(III) ion in a mononuclear Dy/DOTA complex, as confirmed by the calculated orientation of the anisotropic axis.[3a] The results revealed that perturbations of ligand field could affect the local anisotropy of lanthanide ions, resulting in varied SMM behaviours.[3] Inspired by these observations, modulation of ligands upon chemical or physical stimuli, like pH value, light, pressure, temperature, etc.,[4] would be a potential way to change the ligand field, and then further to tune the SMM behaviour of lanthanide complexes.

The optically active ligand, 1,2-bis(4-pyridyl)ethene (bpe) and its derivatives, have been widely used to construct photo-responsive structures because of their facility for photochemical [2+2] cycloaddition (Scheme 1) with formation of cyclobutyl ring.[5,6] Such structural transformation could affect the physicochemical properties of complexes, such as conductivity,[6a] magnetism,[6b] or gas absorption.[6c] However, as far as we know, the study focusing on modulation of SMM behaviour through photodimerization reaction has never been explored.

Scheme 1 The photochemical [2+2] cycloaddition of bpe.

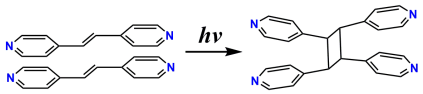

Herein, we report a new Dy(III)-based complex, $[Dy(bpe)(H_2O)_4(NO_3)_2](NO_3)\cdot 2bpe$ (**1**), with bpe as a photo-reactive module. Upon UV irradiation, the coordinated bpe underwent [2+2] transformations, leading to an after-irradiated product, $[Dy_2(tpcb)(H_2O)_8(NO_3)_4](NO_3)_2\cdot 2bpe\cdot tpcb$ (**2**, tpcb = tetrakis(4-pyridyl)cyclobutane). Detailed magnetic measurements on diluted samples, $[Dy_{0.055}Y_{0.945}(bpe)(H_2O)_4(NO_3)_2](NO_3)\cdot 2bpe$ (**1'**) and $[Dy_{0.11}Y_{1.89}(tpcb)(H_2O)_8(NO_3)_4](NO_3)_2\cdot 2bpe\cdot tpcb$ (**2'**) reveal **1'** performs an SMM behaviour while for **2'** a field-induced slow relaxation was observed. The influence of [2+2] cycloaddition on magnetic dynamics is further explained with the help of CASSCF/RASSI calculations.[7a]

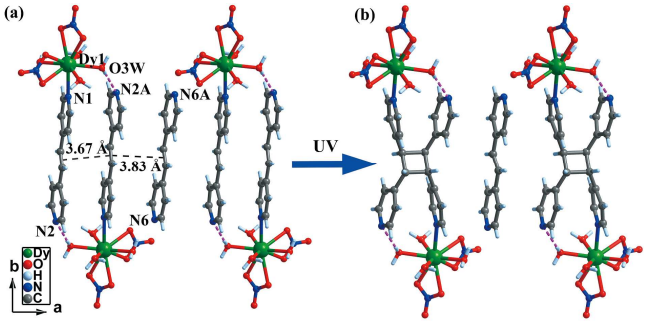

Fig. 1 The [2+2] cycloaddition reaction of the parallel bpe ligands in **1**. The hydrogen bonds are displayed as purple dashed lines.

The reaction of $Dy(NO_3)_3\cdot 6H_2O$ and bpe in a mixture solution of MeCN/EtOH gave colourless rod-like crystals **1**. Complex **1** contains one symmetry-independent Dy(III) ion, which is nine-

[a] *Key Laboratory of Bioinorganic and Synthetic Chemistry of Ministry of Education, School of Chemistry & Chemical Engineering, Sun Yat-Sen University, 510275 Guangzhou, P. R. China. E-mail: ljliang1987@gmail.com; jiajh3@mail.sysu.edu.cn; tongml@mail.sysu.edu.cn*

[b] *Departament de Química Inorgànica and Institut de Recerca de Química Teòrica i Computacional, Universitat de Barcelona, Diagonal 645, E-08028 Barcelona, Spain. E-mail: eliseo.ruiz@qi.ub.es*

† *Electronic supplementary information (ESI) available: Experimental procedures, structure and crystallographic data, physical measurements, computational details. CCDC 1051853 (**1**), 1051854 (**2**), 1401223 (**1'**), 1401224 (**2'**). For ESI and crystallographic data in CIF format see DOI: xxxxxxxx*

coordinated in a NO_8 mode respectively by one terminal-coordinated bpe ligand, two chelated NO_3^- units and four H_2O molecules (Fig. 1a and S3a, ESI†), forming a mononuclear $[Dy(bpe)(H_2O)_4(NO_3)_2]^+$ cation with one NO_3^- as counterion. Two more bpe free ligands were found in space lattice. Along the *c* axis, the cationic motifs are hydrogen bonded with each other through uncoordinated NO_3^- ions, resulting in a supramolecular 1D chain with the minimum inter-mononuclear Dy···Dy distance of 8.41 Å (Fig. S4, ESI†). Each pair of bpe ligands from two neighbouring cations are anchored through the complementary N···H-O hydrogen bonds (ca. 2.79 Å, Fig. 1a). The olefinic bonds are aligned parallel to each other with center-to-center distance of 3.67 Å. Such olefin separation suggests the potential of photochemical [2+2] cycloaddition reaction for **1** (<4.2 Å).[5,6] Besides, another type of packing mode of C=C bonds was also found in **1**. Three guest bpe molecules are closely packed with each other through hydrogen bonding interactions between N atoms of pyridyl groups and O atoms of H_2O molecules and obvious π···π interactions (Fig. S5a, ESI†). The middle bpe molecule locating on the symmetric center adopts a criss-cross alignment of C=C bonds with the other two bpe on both sides. The distance between adjacent C=C centers is 3.49 Å.

UV irradiation of single crystal **1** for 10 hours at room temperature by an ultra-high pressure mercury lamp (*P* = 300 W) afforded **2** in a single-crystal-to-single-crystal (SCSC) manner (Table S1, ESI†). Single-crystal X-ray analysis of **2** reveals the occurrence of a quantitative photodimerization reaction. Every two coordinated bpe ligands took place [2+2] cycloaddition with formation of *rctt* (regio *cis*, *trans*, *trans*)-tpcb while guest bpe molecules remained unreacted due to a relatively longer olefin separation with coordinated bpe ligand (ca. 3.83 Å, Fig. 1a). Thus, a dinuclear **2** formed from the conversion of mononuclear **1** due to the formation of cyclobutane rings (Fig. S3b, ESI†). Accordingly, the coordination environment of Dy(III) center has slightly varied after UV irradiation with detailed bond lengths and bond angles in Table S2 (ESI†). Further *SHAPE* analyses indicate the coordination geometry of Dy(III) center in **2** appears to more deviate from capped square antiprism (C_{4v}) in contrast to **1** (Table S3†). Additionally, for the criss-cross packed bpe ligands, the formation of *rctt*–tpcb (Fig. S5, ESI†) is also observed as a result of the pedal motion of aligned criss-cross C=C groups.[5c]

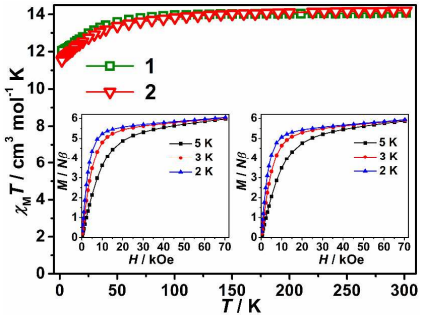

Fig. 2 Temperature-dependent $\chi_M T$ products at 1 kOe for **1** (green) and **2** (red). Inset: plots of *M*–*H* for **1** (left) and **2** (right) at 2, 3 and 5 K. The solid lines are guided by eyes.

Temperature-dependent magnetic susceptibilities were performed in a direct-current (dc) field of 1 kOe (Fig. 2). At room temperature, the $\chi_M T$ values of 13.9 and 14.2 $cm^3 \cdot K \cdot mol^{-1}$ for **1** and **2** respectively, are agreeable with the expected value of one Dy(III) ion (14.2 $cm^3 \cdot K \cdot mol^{-1}$ for the $^6H_{15/2}$ state). Upon cooling, the $\chi_M T$ values of **1** and **2** gradually decrease to 12.0 and 11.5 $cm^3 \cdot K \cdot mol^{-1}$, respectively, indicating the progressive depopulation of Stark sublevels of Dy(III) ion and/or dipolar magnetic interactions. The magnetization at 2 K increases rapidly with magnetic field strength up to about 9 kOe and then increases slowly, finally reaching the "saturation" of 6.05 *Nβ* for **1** and 5.93 *Nβ* for **2** at 70 kOe.

Alternating-current (ac) susceptibility measurements were carried out to study the dynamic behaviour. Under a zero dc field, a relaxation process was found for **1** where the maximum of magnetic susceptibilities χ_M'' was observed at around 1 kHz at 2K, while no maximum of χ_M'' was found for **2**, suggesting the spin-reversal process relaxes faster than **1** (Fig. S7, ESI†). It is possible that the existence of quantum tunnelling of magnetization (QTM) would accelerate the relaxation process. So a series of external dc fields (0-2.0 kOe) were applied for **1** and **2** at 2 K, and a set of peaks in χ_M'' were observed shifting to low frequencies (Fig. S8a-b, ESI†), suggesting the slowing of relaxation processes for both complexes. As the increasing of dc field over 1 kOe, the tails of χ_M'' signals appear to rise again at lower frequency regime (<10 Hz), suggesting onset of a second slower relaxation process. Argand plots of χ_M'' *vs.* χ_M' further indicate the dual-relaxation behaviour above 1.2 kOe dc field, with the emergence of a second semicircle at low frequency (Fig. S9a-b, ESI†).

As we know, dipolar interactions could be responsible for the field-induced dual relaxation behavior.[7] Dilution method was conducted to determine the influence of dipolar interactions due to the presence of hydrogen bonds and close Dy^{3+}···Dy^{3+} distances (8.41 Å for **1** and 8.54 Å for **2**). The magnetic Dy(III) sites of **1** were diluted with diamagnetic Y(III) ions with Dy:Y molar ratio of 1:17 giving product **1'**. Naturally, diluted sample **2'** was then obtained under the UV irradiation of **1'**. Frequency-dependent ac measurements for **1'** and **2'** at various dc field were performed. The low-frequency tails of χ_M'' signals found in **1** and **2** are no longer visible (Fig. S8c-d, ESI†) and the Argand plots show well single semicircles for diluted samples (Fig. S9c-d, ESI†). These results suggest the second relaxation process observed in in **1** and **2** should be caused by dipolar interactions. In this regard, we conclude the slower relaxation process for diluted samples is mainly attributed to the single Dy(III) ion behaviour. Therefore, we are focusing on the dynamic behaviours of **1'** and **2'** to investigate the influence of coordination sphere on magnetic response of Dy(III) ion.

A set of visible peaks in χ_M'' signals characterizing the SMM behaviour are observed for **1'** under a zero dc field (Fig. 3a). The relaxation time (τ) was extracted by fitting Cole-Cole data in the range of 1.8-7.0 K with a generalized Debye model (Fig. S11a, ESI†). The distribution coefficient values (α) are 0.049-0.49. Fitting high-temperature data with an Arrhenius law gave the energy barrier $\Delta = 38.3$ cm^{-1} and $\tau_0 = 9.81 \times 10^{-9}$ s (Fig. 3d).

Applying an optimum field of 300 Oe which leads to the slowest magnetization relaxation, the peaks of χ_M'' signals at various temperatures were shifted to the lower frequency region compared with that at a zero field (Fig. 3b). This is indicative of the reduced QTM effect by applying a dc field. Values of Δ and τ_0 were estimated to be 39.4 cm^{-1} and 8.92 × 10^{-9} s, respectively (Fig. 3d).

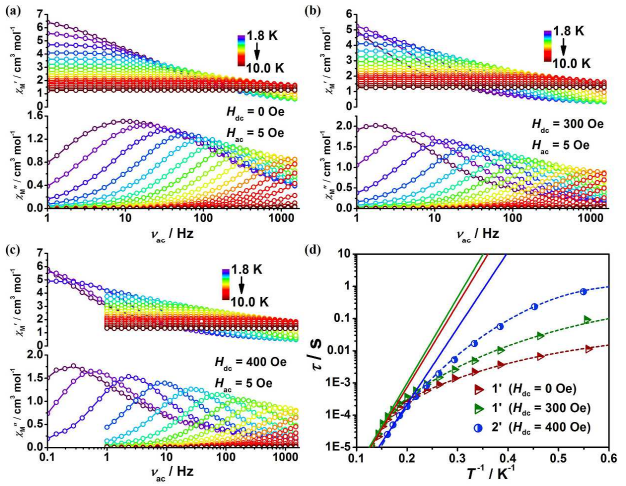

Fig. 3 The frequency-dependent ac susceptibilities for diluted samples **1'** at zero (a) and 300 Oe (b) dc fields, and **2'** under a 400 Oe dc field (c). The τ vs T^{-1} plot (d) for **1'** under zero (red) and 300 (green) Oe fields; for **2'** under a 400 Oe dc field (purple), the solid and dashed lines represent the best fits by Arrhenius law and eqn (**1**), respectively.

For **2'**, a visible change of the relaxation behaviour was found. In the absent of dc field, only a peak was observed at 1488 Hz at 2 K, suggesting the relaxation process in **2'** is faster than **1'** (Fig. S8b, ESI†). However, under an optimum field of 400 Oe, the peaks of χ_M'' signals shown in whole measured frequencies (0.1-1488 Hz, Fig. 3c) means the relaxation time of **2'** is obviously enlarged. The τ values obtained from Cole-Cole plots (Fig. S13, ESI†) further confirm such observation, *e.g.* at 1.8 K, the τ = 0.68 s for **2'** is about seven times larger than τ = 0.09 s for **1'** (Tables S4-S6, ESI†). The energy barrier extracted from high-temperature data by Arrhenius law was estimated to be 33.3 cm^{-1} with the preexponential factor $\tau_0 = 1.22 \times 10^{-9}$ s (Fig. 3d).

In order to get further insight into the low-lying electronic structure and the magnetic anisotropy on the Dy(III) site, *ab initio* calculations of the CASSCF(7,9)/RASSI type (Molcas 8.0 code)[8] for three different multiplicities (21, 128 and 98 states for sextet, quartet and doublet calculations, respectively) on the experimental structures were performed while the employed basis set has the following contractions: Dy [9s8p6d4f3g2h]; O [4s3p2d1f]; N [4s3p2d1f]; C [3s2p]; H [2s].[9] For **2**, the calculation was performed replacing one of the Dy^{III} centers by diamagnetic La(III) cations (using model potentials). The calculated *g*-factors clearly show the large anisotropic character of these systems (g_x, g_y, g_z **1**: 0.17, 0.33, 19.09; **2**: 0.35, 0.98, 18.4). The shape of the plotted beta density of the 4*f* Dy^{III} electrons obtained in the CASSCF step for the ground state of the two complexes is represented in Fig. 4 (Dy^{III} centers have $4f^9$ electron configuration and the 7 alpha electrons give an isotropic spherical electron density),[10] showing the relatively large distortion of the beta electron density of the oblate shape[2b] despite of the relatively large calculated magnetic anisotropy. The direction of the magnetic moment is slightly different between the two complexes (Fig. 4) but is more or less aligned towards the axial nitrato ligand reflecting a larger metal-ligand electron repulsion in such direction due to the negative charge of nitrato ligand.[10,11]

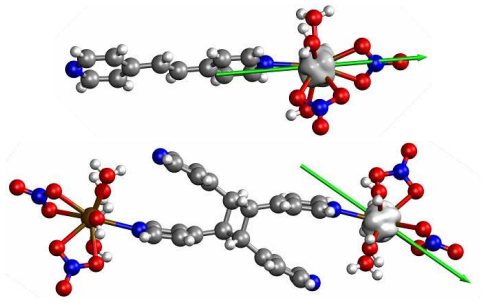

Fig. 4 Beta spin density isosurface of the Dy(III) f electrons for the spin-free CASSCF and the direction of the magnetic moment of the ground state is indicated as a green arrow for **1** (above) and **2** (below).

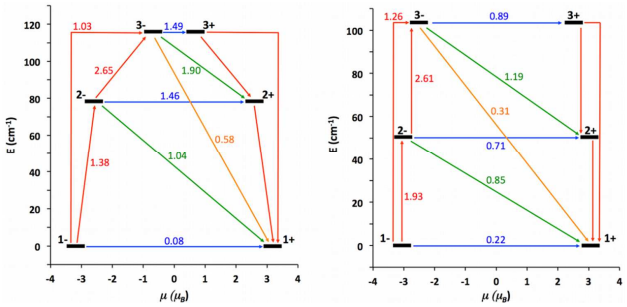

Fig. 5 Lowest three Kramers doublets and ab initio computed relaxation mechanism in **1** (left) and **2** (right). The thick black lines imply KDs as a function of their magnetic moment along the main anisotropy axis. Red lines indicates magnetization reversal mechanism The blue lines correspond to ground state QTM and thermally assisted-QTM via the first and second excited KDs, green (and orange) lines show possible Orbach relaxation processes. The values close to the arrows indicate the matrix elements of the transition magnetic moments (above 0.1 is expected an efficient spin relaxation mechanism).

The calculated energies of the Kramers doublets (KDs) are represented in Fig. 5. The spin relaxation mechanisms indicate an efficient relaxation through the first excited state and we obtained the first excitation energy with 78.4 cm^{-1} for **1** while 50.5 cm^{-1} for **2**.[12] Obviously, the calculated energies of excited Kramers doublets are relatively larger than the values obtained by Arrhenius fitting, which suggested the Orbach processes for both diluted compounds exist in higher temperature region and the temperature region measured here (1.8-7 K) may dominated by other faster relaxation mechanism. In fact, the τ *vs*. $1/T^{-1}$ curves for **1'** and **2'** in Fig. 3d still bend down in the high temperature region, which means that the Arrhenius regime should show up at higher temperatures. The analysis of the spin relaxation mechanism (Fig. 5) reveals a larger tunneling effect at ground state level for **2** consistent with the

requirement for **2'** of magnetic field to present SMM behaviour while **1'** is a zero-field SMM system (also it is noticed in the previously reported larger calculated g_x and g_y values for **2**).[10] The calculated ground state magnetic moment is consistent with a major m_J = 15/2 contribution and it is slightly larger for **1** in agreement with the experimental magnetization (Fig. 2).

In light of the observed curvature of the Arrhenius plot at low temperature, a non-negligible influence of Direct and/or Raman processes should be considered for determining the relaxation rate. The temperature-dependent relaxation times for diluted systems were analysed by the following equation.[14,15]

$$\tau^{-1} = A_1H^3\coth(A_2H/T) + B_1/(1 + B_2H^2) + CT^n + \tau_0^{-1}\exp(-\Delta/k_BT) \quad (1)$$

In eqn (1), four terms represent direct, QTM, Raman, and Orbach processes, respectively. In order to avoid overparameterisation, parameters of A_1, A_2, B_1, and B_2 were fixed with values extracted from the nonlinear fitting of field-dependent relaxation data (Fig S14, ESI†), as well as Δ in Orbach term replaced by values from *ab initio* calculations. Consequently, a satisfied fit respectively for **1'** and **2'** was performed (Fig. 3d and Table S7, ESI†). We noted that the Raman exponent for **2'** with n = 8.94 was agreement with a pure two phonon Raman process (n = 9 for Kramer ions, and n = 7 for non-Kramers ions).[16] For **1'**, the resulting n value for Raman term equals to 3.92 and 5.44 at zero and 300 Oe fields, respectively. The growing n values from **1'** to **2'** indicate the different contributions/mechanisms of Raman process. Moreover, comprehensive maps of contribution from each relaxation process were drawn (Fig. S15, ESI†). It is obvious that Raman relaxation process is dominated at a wide temperature, further suggesting the existence of Orbach process at higher temperature for **1'** to **2'**.

In conclusion, a new photo-responsive Dy(III)-based SMM was reported. Upon UV irradiation, a magnetic transformation from the SMM behaviour (**1'**) to a field-induced slow relaxation (**2'**) occurred through the [2+2] cycloaddition of bpe ligands. As confirmed by CASSCF/RASSI calculations, subtle perturbations of coordination sphere around Dy(III) ions actually affect the magnetic anisotropy of Dy(III) centre, leading to such different magnetic behaviours. This work not only establishes the usefulness of photodimerized [2+2] cycloaddition reaction for modulating magnetic behaviours in SMMs, but also provides a means to design and modify the multifunctional SMMs. The attempt to realize a reversible [2+2] cycloaddition reaction in SMMs is on progress.

This work was supported by the "973 Project" (2012CB821704 and 2014CB845602), the NSFC (Grant nos 91122032, 91422302 and 21301197) and the NSF of Guangdong (S2013020013002). It was also supported by the Spanish Ministerio de Economía y Competitividad (grants CTQ2011-23862-C02-01). E.R. thanks Generalitat de Catalunya for an ICREA Academia fellowship also CSUC for computer time.

Notes and references

1 (a) R. Vincent, S. Klyatskaya, M. Ruben, W. Wernsdorfer and F. Balestro, *Nature*, 2012, **488**, 357; (b) M. Urdampilleta, S. Klyatskaya, J-P. Cleuziou, M. Ruben and W.Wernsdorfer, *Nat. Mater.*, 2011, **10**, 502; (c) A. Ardavan, O. Rival, J. J. L. Morton, S. J. Blundell, A. M. Tyryshkin, G. A. Timco and R. E. P. Winpenny, *Phys. Rev. Lett.*, 2007, **98**, 057201-1;

2 (a) D. N. Woodruff, R. E. P. Winpenny and R. A. Layfield, *Chem. Rev.*, 2013, **113**, 5110; (b) J. D. Rinehart and J. R. Long, *Chem. Sci.*, 2011, **2**, 2078; (c) J.-L. Liu, J.-Y. Wu, Y.-C. Chen, V. Mereacre, A. K. Powell, L. Ungur, L. F. Chibotaru, X.-M. Chen and M.-L. Tong, *Angew. Chem. Int. Ed.*, 2014, **53**, 12966.

3 (a) G. Cucinotta, M. Perfetti, J. Luzon, M. Etienne, P.-E. Car, A. Caneschi, G. Calvez, K. Bernot and R. Sessoli, *Angew. Chem. Int. Ed.*, 2012, **51**, 1606; (b) F. Habib, J. Long, P.H. Lin, I. Korobkov, L. Ungur, W. Wernsdorfer, L. F. Chibotaruc and M. Murugesu, *Chem. Sci.*, 2012, **3**, 2158; (c) K. S. Pedersen, L. Ungur, M. Sigrist, A. Sundt, M. Schau- Magnussen, V. Vieru, H. Mutka, S. Rols, H. Weihe, O. Waldmann, L. F. Chibotaru, J. Bendix and J. Dreiser, *Chem. Sci.*, 2014, **5**, 1650.

4 (a) N. Ishikawa, Y. Mizuno, S. Takamatsu, T. Ishikawa and S. Koshihara, *Inorg. Chem.*, 2008, **47**, 10217; (b) D. Pinkowicz, M. Ren, L. M. Zheng, S. Sato, M. Hasegawa, M. Morimoto, M. Irie, B. K. Breedlove, G. Cosquer, K. Katoh and M. Yamashita, *Chem. Eur. J.*, 2014, **20**, 12502.

5 (a) Y.-C. Ou, W.-T. Liu, J.-Y. Li, G.-G. Zhang, J. Wang and M.-L. Tong, *Chem. Commun.*, 2011, **47**, 9384; (b) M. Nagarathinam and J. J. Vittal, *Chem. Commun.*, 2008, **4**, 438; (c) I.-H. Park, R. Medishetty, J.-Y. Kim, S. S. Lee and J. J. Vittal, *Angew. Chem. Int. Ed.*, 2014, **53**, 5591.

6 (a) K. M. Hutchins, T. P. Rupasinghe, L. R. Ditzler, D. C. Swenson, J. R. G. Sander, J. Baltrusaitis, A. V. Tivanski and L. R. MacGillivray, *J. Am. Chem. Soc.*, 2014, **136**, 6778; (b) X.-Y. Wang, Z.-M. Wang and S. Gao, *Chem. Commun.*, 2007, **11**, 1127; (c) H. Sato, R. Matsuda, M. H. Mira and S. Kitagawa, *Chem. Commun.,* 2012, **48**, 7919.

7 (a) K. R. Meihaus, J. D. Rinehart and J. R. Long, *Inorg. Chem.*, 2011, **50**, 8484; (b) K. R. Meihaus, J. D. Rinehart and J. R. Long, *J. Am. Chem. Soc.*, 2010, **132**, 7572; (c) P.-E. Car, M. Perfetti, M. Mannini, A. Favre, A. Caneschi and R. Sessoli, *Chem. Commun.*, 2011, **47**, 3751; d) M. Ren, S.-S. Bao, R. A. S. Ferreira, L.-M. Zheng and L. D. Carlos, *Chem. Commun.*, 2014, **50**, 7621.

8 F. Aquilante, L. De Vico, N. Ferre, G. Ghigo, P. A. Malmqvist, P. Neogrady, T. B. Pedersen, M. Pitonak, M. Reiher, B. O. Roos, L. Serrano-Andres, M. Urban, V. Veryazov and R. Lindh, *J. Comput. Chem.*, 2010, **31**, 224.

9 (a) L. Ungur and L. F. Chibotaru, *Phys. Chem. Chem. Phys.*, 2011, **13**, 20086. (b) L. F. Chibotaru and L. Ungur, *J. Chem. Phys.*, 2012, **137**, 064112.

10 D. Aravena and E. Ruiz, *Inorg. Chem.*, 2013, **52**, 13770.

11 N. F. Chilton, D. Collison, E. J. L. McInnes, R. E. P. Winpenny and A. Soncini, *Nat. Commun.*, 2013, **4**, 2551.

12 J. Ruiz, A. J. Mota, A. Rodriguez-Dieguez, S. Titos, J. M. Herrera, E. Ruiz, E. Cremades, J. P. Costes and E. Colacio, *Chem. Commun.*, 2012, **48**, 7916.

13 S. Gómez-Coca, D. Aravena, R. Morales and E. Ruiz, *Coord. Chem. Rev..*, 2015, **289**, 379.

14 (a) J. M. Baker and N. C. Ford, *Phys. Rev.*, 1964, **136**, 1692; (b) G. H. Larson and C. D. Jeffries, *Phys. Rev.*, 1966, **145**, 311.

15 (a) J. M. Zadrozny, M. Atanasov, A. M. Bryan, C.-Y. Lin, B. D. Rekken, P. P. Power, F. Neese and J. R. Long, *Chem. Sci.*, 2013, **4**, 125; (b) E. Lucaccini, L. Sorace, M. Perfetti, J. P. Costes and R. Sessoli, *Chem. Commun.*, 2014, **50**, 1648.

16 (a) A. Singh and K. N. Shrivastava, *Phys. Status Solidi B*, 1979, **95**, 273; (b) K. N. Shrivastava, *Phys. Status Solidi B*, 1983, **117**, 437; (c) J.-L. Liu, Y.-C. Chen, Y.-Z. Zheng, W.-Q. Lin, L. Ungur, W. Wernsdorfer, L. F. Chibotaru and M.-L. Tong, *Chem. Sci.*, 2013, **4**, 3310.

TOC: The first example of phototunable SMM has been reported. Upon UV irradiation, the remarkable variations of coordination sphere of Dy(III) ions actually affect the magnetic behaviour of compound, leading to a magnetic transformation from the SMM behaviour to a field-induced slow relaxation through SCSC [2+2] cycloaddition reaction.